Taylor & Francis
Taylor & Francis Group

Transportation Letters
The International Journal of Transportation Research

ISSN: (Print) (Online) Journal homepage: https://www.tandfonline.com/loi/ytrl20

Investigation of car-following models in disordered traffic using trajectory data obtained from unmanned aerial vehicles

Madhuri Kashyap N R, Kalaanidhi Sivagnanasundaram, Venkatesan Kanagaraj, Gowri Asaithambi & Tomer Toledo

To cite this article: Madhuri Kashyap N R, Kalaanidhi Sivagnanasundaram, Venkatesan Kanagaraj, Gowri Asaithambi & Tomer Toledo (2023) Investigation of car-following models in disordered traffic using trajectory data obtained from unmanned aerial vehicles, Transportation Letters, 15:8, 834-844, DOI: 10.1080/19427867.2022.2099150

To link to this article: https://doi.org/10.1080/19427867.2022.2099150

Published online: 13 Jul 2022.

Submit your article to this journal

Article views: 434

View related articles

View Crossmark data

Citing articles: 1 View citing articles

Full Terms & Conditions of access and use can be found at
https://www.tandfonline.com/action/journalInformation?journalCode=ytrl20

TRANSPORTATION LETTERS
2023, VOL. 15, NO. 8, 834–844
https://doi.org/10.1080/19427867.2022.2099150

Taylor & Francis
Taylor & Francis Group

Check for updates

Investigation of car-following models in disordered traffic using trajectory data obtained from unmanned aerial vehicles

Madhuri Kashyap N R[a], Kalaanidhi Sivagnanasundaram[b], Venkatesan Kanagaraj[c], Gowri Asaithambi[a] and Tomer Toledo[b]

[a]Department of Civil and Environmental Engineering, Indian Institute of Technology Tirupati, Tirupati, India; [b]Research Scholar Department of Civil and Environmental Engineering, Technion - Israel Institute of Technology, Haifa, Israel; [c]Department of Civil Engineering, Indian Institute of Technology Kanpur, Kanpur, India

ABSTRACT

Car-following models are the cornerstones of microscopic traffic simulation tools and intelligent transportation systems, but the applicability of car-following models to disordered traffic have not been investigated in detail with longer trajectory dataset. To address this gap, two car-following models namely, Intelligent Driver Model (IDM) and Full Velocity Difference Model (FVDM) are calibrated using trajectory data collected on an urban arterial road in Chennai, India using Unmanned Aerial Vehicles. The raw data are smoothed for noise removal and the car-following pairs are identified based on the lateral overlap and following duration. The models are calibrated by minimizing the deviations between the observed and simulated longitudinal gaps between leader and follower using genetic algorithm. The obtained errors are between 2.5% and 19.5%, which are comparable with standard ranges of error reported in literature. The optimal parameter values represent the distinct characteristics of disordered traffic in comparison with the homogeneous traffic.

KEYWORDS

Calibration; car following models; disordered traffic; unmanned air vehicles; trajectory data

Introduction and background

Microscopic traffic flow models are commonly used to explain collective phenomena such as traffic instabilities, breakdowns, and propagation of stop-and-go waves. Car-following models capture the longitudinal dynamics of vehicles and describe the actions of individual vehicles in response to the surrounding traffic. The earlier car-following models are categorized as stimulus-response models, psychophysical models, and collision avoidance models (Brackstone and McDonald 1999). The stimulus-response models were developed to predict the response of the follower to the stimuli with respect to leader, i.e., change in headway and relative speeds. General Motors (GM) car-following model (Chandler, Herman, and Montroll 1958) and its variant models (May and Keller 1967; Heyes and Ashworth 1972) are the notable stimulus response models. The safety-distance models or collision-avoidance models (Kometani 1959) are built upon the assumption that the follower tries to maintain a safe distance with the leader and adapts its speed accordingly to avoid collision. Gipps model (Gipps 1981) is the mostly used collision avoidance car-following model, especially for microsimulation of traffic. Psychophysical models are developed based on the assumption that the actions performed by the drivers are based on their ability to perceive the relative speeds and relative distance with the vehicle ahead (Wiedemann 1974). Other car-following models, including optimal velocity models and desired measures models, have gained popularity in modeling vehicular movements due to their simple formulations and realistic outcomes. Optimal velocity model (OVM) assumes that the follower maintains an optimal speed dependent on the relative distance with the leader. The acceleration of follower is based on the deviation from its optimal speed (Bando et al. 1995). There are different versions of OVM such as two velocity difference model (Ge at al., 2008) and full velocity difference model (Jiang, Wu, and Zhu 2001; Jin et al. 2010). The intelligent driver model (IDM) is a desired distance model developed based on the assumption that the drivers perform actions (acceleration) due to the difference between their current state of motion and their desired state such as speed, spacing, etc. (Treiber, Hennecke, and Helbing 2000). IDM is a collision-free model in a single lane traffic with continuously differentiable acceleration function.

Car-following models are developed based on specific assumptions on driving behavior and each model has a specific set of parameters which should be identified accurately to use for practical purposes. Calibration is the approach to obtain the set of parameters that minimizes the difference between the observed and model predicted values. Several attempts have been made to calibrate different car-following models under homogeneous traffic conditions as seen in developed countries (Brackstone and McDonald 1999; Ossen and Hoogendoorn 2005; Brockfeld and Wagner 2005; Kesting and Treiber 2008; Kurtc 2020). Drivers in different countries drive different types of vehicles, have different driving styles, and are bound by different traffic regulations and driving cultures (Treiber and Kesting 2013; Daamen, Campanella, and Hoogendoorn 2013). For example, disordered traffic (e.g., Indian traffic) is characterized by wide variations in the operating characteristics of vehicles, weak lane discipline, aggressive driving, large diversity in driver behavior, inadequate road design, poor access management, presence of roadside side frictions (e.g., bus stops, on-street parking) dynamic effective road width, and continuous vehicular entry, exit and turns. The weak lane discipline provides additional degree of freedom for vehicular movement (both lateral and longitudinal components for the position, velocity, and acceleration) and results in significant inter-/intra-vehicular interactions. Hence, a car-following model that works well for homogeneous traffic may not perform well when applied to disordered traffic.

CONTACT Madhuri Kashyap N R ce19d003@iittp.ac.in Research Scholar Department of Civil and Environmental Engineering, Indian Institute of Technology Tirupati

© 2022 Informa UK Limited, trading as Taylor & Francis Group

Nevertheless, some of the researchers made attempt to calibrate few car-following modes for disordered traffic conditions (Asaithambi et al. 2018; Raju, Arkatkar, and Joshi 2020).

The data for calibration of car-following models are obtained from various sources such as field observations (NGSIM 2005; Kanagaraj et al. 2015; Krajewski et al. 2018), driving experiments (Ranjitkar, Nakatsuji, and Kawamua 2005) and instrumented vehicles (Kesting and Treiber 2008) in homogeneous and disordered traffic. After the selection of data collection method, defining the measure of performance (MoP) and goodness of fit (GoF) and the choice of optimization algorithm plays a significant role in the calibration process. MoP is the variable that characterizes the car-following behavior and its field observed values are compared with the values obtained by the calibrated model. The spacing between leader and follower (leader's back bumper to follower's front bumper) was chosen as the MoP in previous studies (Kesting and Treiber 2008; Kurtc 2020). The optimization algorithms such as genetic algorithm, interior point algorithm, simulated annealing, downhill simplex, and optquest/multistart are the commonly used optimization algorithms to calibrate car-following models (Ranjitkar, Nakatsuji, and Kawamua 2005; Kesting and Treiber 2008; Raju, Arkatkar, and Joshi 2020; Kurtc 2020). Among the different algorithms, Genetic Algorithm is the most used because it can prevent local minima and reach the global optimum with a stochastic global search method (Saifuzzaman et al. 2015). In most of the previous studies, car-following models are customarily calibrated using macroscopic traffic data (e.g., speed, density) instead of microscopic data, leading to a loss of accuracy and realism (Ravishankar and Mathew 2011; Asaithambi et al. 2018).

With the above motivation, the main aim of the study is to systematically calibrate two car-following models, namely, Intelligent Driver Model (IDM) and Full Velocity Difference Model (FVDM) under disordered traffic using trajectory data. For this purpose, traffic data are collected from a road stretch of length 605 m, located on an urban arterial road in Chennai city (India). The optimal parameters of this model will be determined using a non-linear optimization technique, genetic algorithm. Three types of error measures are considered since the fit errors may not work as a good base for the assessment of models. Moreover, it is decided to minimize the objective function with respect to vehicle gaps since it automatically reduces the average speed errors. This study will provide better insights on vehicle-following behavior of drivers in disordered traffic and determining the best model for use in disordered traffic.

In the next section, the two car-following models under investigation is discussed. The third section presents the details of data collection, extraction of trajectory data and its smoothing procedure. In the fourth section, the methodological approach for the non-linear optimization problem is described. Fifth section discusses the results of the work followed by section on conclusions and an overview for further work.

Car-following models under investigation

Car-following models are used to reproduce the longitudinal dynamics of vehicles which model the actions such as acceleration and deceleration of each driver as a response to the neighboring traffic and includes various regimes such as free flow, following the leader, and approaching standing vehicles. In this study, two car-following models such as IDM and FVDM, the widely used models in previous studies, are considered for calibration. These models are formulated as ordinary differential equations and, subsequently, time and space are treated as continuous variables, and characterized by an acceleration function, $\dot{v} = \frac{dv}{dt}$ which depends on real speed v(t), gap s(t) and speed difference with the leader Δv(t).

$$\dot{v}(s, v, \Delta v) = f(s, v, \Delta v) \tag{1}$$

Intelligent driver model

Intelligent driver model gives acceleration of the follower as an output, which is dependent on driver's desired measures (desired speed and desired distance with respect to leader). IDM is capable of modeling different driving regimes such as accelerating from standstill, following, approaching and free flow. The general mathematical formulation of the IDM model is:

$$\dot{v} = a\left[1 - \left(\frac{v}{v_0}\right)^{\delta} - \left(\frac{s^*(v, \Delta v)}{s}\right)^2\right] \tag{2}$$

This formulation combines: 1) acceleration strategy $\dot{v_{free}} = a\left[1 - \left(\frac{v}{v_0}\right)^{\delta}\right]$ for a desired speed (v_0) on a free road with maximum acceleration (a) as the parameter, and 2) a braking strategy $\dot{v_{brake}} = -a\frac{s^*}{s}$ which dominates if the current gap (s) is lesser than the desired minimum gap:

$$s^*(v, \Delta v) = s_0 + \max\left(0, vT + \frac{v\Delta v}{2\sqrt{ab}}\right) \tag{3}$$

where

$\dot{v}$ = *Acceleration of the follower*, a = *Maximum acceleration*,
v = *Speed of the follower*,
v_0 = *Desired speed*,
s^* = *Desired distance*,
s = *Longitudinalgapbetweenleaderfollower*,
Δv = *Speed difference with the leader*, s_0 = *Minimum spacing*,
T = *Desired or safety time gap*, b = *Comfortable deceleration*

Minimum spacing (s_0) in congested traffic is only dominant when speeds are low. In equation 3, the dominating term is vT in stationary traffic that correlates to following the leader maintaining a constant desired time gap T. The final term is dominant only in non-stationary traffic and executes an intelligent driving behavior as well as a braking approach which, mainly in all situations, limits braking deceleration to the comfortable deceleration. Nevertheless, IDM brakes stronger than b when the gap becomes too small. All the IDM parameters (v_0, T, s_0, a, b) are characterized by positive values.

Full velocity difference model

Full velocity difference model is an extended version of optimal velocity model. In this model, follower's acceleration depends on the optimal velocity which is a function of spacing $v_{opt}(s)$) and speed difference with the leader *Δv*. The mathematical description of FVDM is given as:

$$\dot{v} = \frac{v_{opt}(s) - v}{\tau} - \gamma\Delta v \tag{4}$$

where τ = adaptation time, which explains the adaptation to a new speed due to changes in v and s. The important influence of Δv is captured by the sensitivity parameter λ.

$$v_{opt}(s) = v_0\frac{\tanh\left(\frac{s}{\Delta s} - \beta\right) + \tanh\beta}{1 + \tanh\beta} \tag{5}$$

where

$\dot{v} = Acceleration\ of\ the\ follower,\ v = Speed\ of\ the\ follower,$
$v_{opt}(s) = Optimal\ velocity\ of\ the\ follower,$
$\tau = Adaption\ time,$
$\Delta s = Transition\ width, \Delta v = Speed\ difference\ with\ the\ leader,$
$v_o = Desired\ speed,\ \beta = Form\ factor, -$
$\gamma = Sensitivity\ to\ speed\ difference,$
$s = Longitudinal\ gap\ between\ leader\ \dot{}follower.$

The parameter v_0 describes the desired speed in free flow traffic conditions. Transition width Δs determines the transition regime varies from $v_{opt} \to 0$ to $v_{opt} \to v_0$ if the distance to the leader turns out to be large. In contrast to the IDM, the FVDM is not completely an accident-free model.

Trajectory data collection and extraction

The trajectory data are found to be a very good source of microscopic traffic data. The process of data collection and extraction in the present study is described in the following subsections:

Study section

The road section selected for this study is located on an urban arterial (six-lane divided) road namely Rajiv Gandhi Salai in Chennai city, India. Length of the study stretch is 700 m of which 605 m (upto the stop line of the downstream intersection which is signalized) are covered in the video as illustrated in Figure 1(a).

Data collection using unmanned aerial vehicles

In this study, it is proposed to track vehicles on a longer section to capture their behavior under different traffic situations. For this purpose, we have used DJI Phantom 4 Pro unmanned aerial vehicles (UAVs) to capture the vehicles from a top-view. Four UAVs were deployed to cover 605 m in such a way that sufficient overlapping of 15–30 m is ensured between any successive UAVs which will help to stitch the trajectories of vehicles (Figure 1b). The traffic videos were recorded in March 2018 with a resolution of 4 K (4096 x 2160). The video survey was conducted by flying the drones in six flights of 15–18 minutes each. In total, around 1.5 hours of data was obtained excluding the take-off, routing and landing times and hence, the data collection process was not continuous (in each flight 15 minutes data is continuous). To ensure the stable recording, drones with gimble support are deployed thereby limiting their hovering and rotations.

Trajectory data extraction

As a first step of trajectory data extraction, the raw videos need to be stabilized. The base frames are the first frames of each camera, and they are rotated in such a way that the road alignment matches the horizontal axis of the frame. Then, the rest of the frames are matched with their respective base frame using feature detection algorithm for which SURF technique of OpenCV (Bradski and Kaehler 2008) is adopted. A perspective homograph matrix for each frame is estimated based on the matched features and they are used for stabilizing the frames.

Once the videos are stabilized, the vehicle trajectories are extracted independently from all the four cameras using a semi-automated extraction tool that is developed using MultiTracker algorithm of OpenCV (Bradski and Kaehler 2008). The algorithm requires drawing bounding boxes around each vehicle in one frame and for the successive frames, the vehicles will be tracked automatically as shown in Figure 2. In case of tracking failure, the algorithm enables us to interfere and draw a new bounding box from the failed frame. The extracted data consist of vehicle ID (independent across cameras), frame number, vehicle type, length, width, longitudinal, and lateral position of vehicles.

Coordinate mapping and stitching

The extracted trajectory data of vehicles which are in image coordinates must be converted to real world coordinates. For this purpose, 60 ground control points are obtained from a total station survey on the site. The base images of all the cameras are imported to ArcGIS and georeferenced using the ground control points. From the stitched image, a control point from each corner of each camera is established and they are used to estimate the homograph matrix independently for each camera using the following formula:

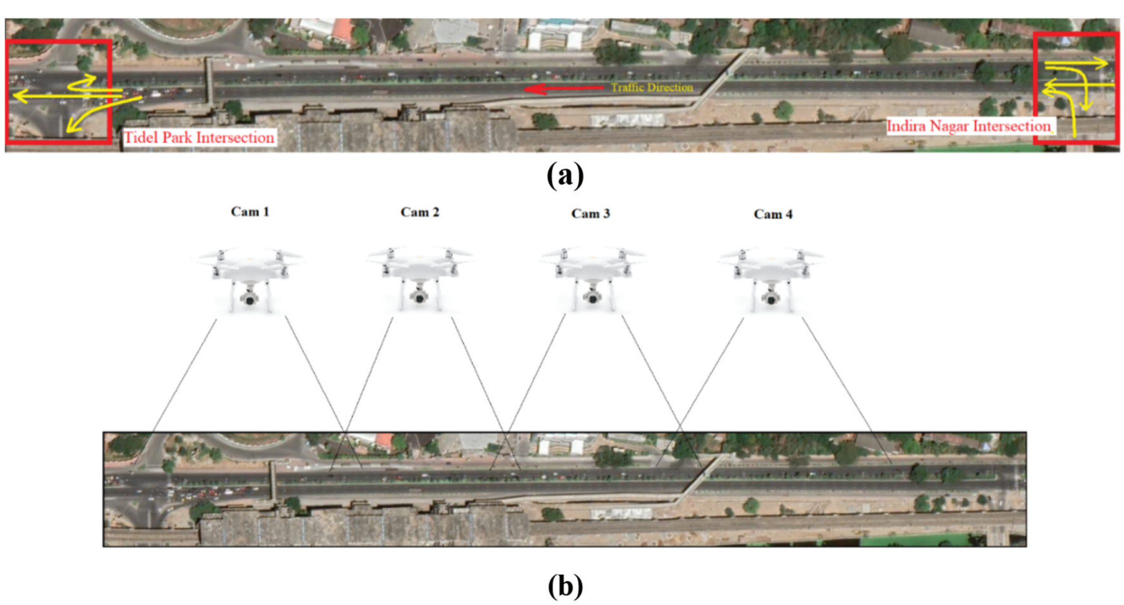

Figure 1. (a) Layout of the study stretch (b) Pictorial representation of the video data collection set-up using four drone cameras.

Figure 2. Snapshot of vehicle tracking process.

$$x_{real} = \frac{h_{11}*x_{image} + h_{12}*y_{image} + h_{13}}{h_{31}*x_{image} + h_{32}*y_{image} + 1} \quad (6)$$

$$y_{real} = \frac{h_{21}*x_{image} + h_{22}*y_{image} + h_{23}}{h_{31}*x_{image} + h_{32}*y_{image} + 1} \quad (7)$$

where h_{ij} are parameters to be estimated. With the estimated matrices, the extracted data of vehicles are converted from image pixels to ground coordinates.

The starting time of recording of all the four cameras were not exactly same and the lag times between all successive cameras were found out. With these lag times, the vehicles' lateral, and longitudinal positions were matched on the overlapping sections and vehicle IDs were replaced by that of the matching vehicle of another camera. Thus, the trajectories of same vehicles across the cameras were stitched together.

Trajectory smoothing

The extracted trajectory data generally contain measurement errors which are interpreted as random noise on the positional location of vehicles and these errors may be further magnified in the differentiation process when estimating the values of speeds and acceleration. From Figure 3, it can be observed that most of the acceleration values calculated from raw data are beyond ±6 m/s^2 due to small time step which indicates that the driver is evidently changing between hard acceleration and hard deceleration within a second, which seems to be unrealistic. The speeds also demonstrate an unrealistic behavior, which shows that drivers do not smoothly accelerate or decelerate. Hence, once the position data are extracted, they need to be smoothed to overcome missing observations to minimize the instantaneous peaks in the raw data.

In the present study, the symmetric exponential moving average filter (sEMA) was used to smoothen the raw data (Thiemann, Treiber, and Kesting 2008). In comparison with moving average smoothing, sEMA performs better, as the weightage given to a data point decreases with increase in its distance from the smoothing window center. Also, sEMA has lesser number of parameters in comparison with Kalman filter (Zheng et al. 2020).

Let $x_\beta(t_i)$ denotes the observed position of vehicle β at time t_i, where i = 1 . . . N_β and N_β indicates the number of data points in the trajectory. The smoothing operation is performed by using data point indices rather than times because the data points are equidistant in time with interval (dt). The smoothing kernel is given by $g(t) = \exp\left(\frac{-t}{T}\right)$, where T indicates smoothing width. The smoothed positions, $\overline{x_\beta}$ are expressed as:

$$\bar{x}_\beta(t_i) = \frac{1}{z}\sum\nolimits_{k=i-D}^{i+D} x_\beta(t_k)e^{-\frac{|i-k|}{\Delta}} \quad (8)$$

where

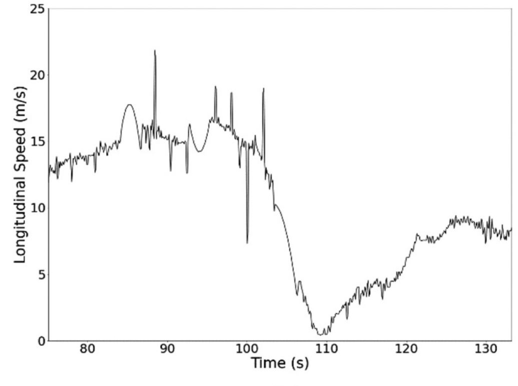

(a)

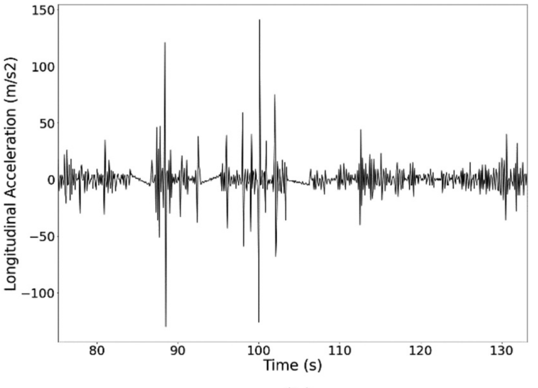

(b)

Figure 3. Problems of raw data: a) Speed profile, and b) Acceleration profile.

$$z = \sum_{k=i-D}^{i+D} e^{-|i-k|/\Delta} \tag{9}$$

$\bar{x}_\alpha(t_i) = Smoothed\ position\ for\ vehicle\ \beta\ at\ time\ step\ t_i$,
$i = 1, 2, \ldots . N_\beta$,
$N_\beta = No.\ of\ data\ points\ in\ vehicle\ \beta's\ trajectory$, $t_k, \Delta = \frac{T}{dt}$,
$T = Smoothing\ width$,

$x_\beta(t_k) = Observed\ or\ recorded\ position\ of\ vehicle\ \beta\ at\ time\ step$,

$dt = Timeintervalbetweendatapointsof trajectory(1/10s)orsamplingrate$,

$D = Smoothing\ window\ width = min\ \{\ 3\Delta,\ i-1,\ N_\alpha - 1\ \}$

The same smoothing width T can be applied to all data sets, and Δ is the equivalent smoothing width measured in data points for the particular data set. Smoothing window width (D) is selected as three times as the smoothing kernel width for any data point which is not closer to the trajectory boundary. For the points closer to the boundaries, the smoothing width is decreased to ensure that the smoothing width is always symmetric.

After performing the smoothing mechanism, smoothed positions will be obtained and then, differentiated to obtain speeds and accelerations using central difference method as follows:

$$V_\beta(t_i) = \frac{X_\beta(t_i + dt) - X_\beta(t_i - dt)}{2dt} \tag{10}$$

$$A_\beta(t_i) = \frac{X_\beta(t_i + dt) - 2X_\beta(t_i) + X_\beta(t_i - dt)}{dt^2} \tag{11}$$

where

$$X_\beta(t_i - dt) = Position\ of\ vehicle\ \beta\ at\ time\ stepst_i - dt.$$

$$X_\beta(t_i) = Position\ of\ vehicle\ \beta\ at\ time\ steps\ t_{i,}$$

$$X_\beta(t_i + dt) = Position\ of\ vehicle\ \beta\ at\ time\ steps\ t_i + dt.$$

$$V_\beta(t_i) = Speed\ of\ vehicle\ \beta\ at\ time\ step\ t_i$$

$$A_\beta(t_i) = Acceleration\ of\ vehicle\ \beta\ at\ time\ step\ t_i$$

.

Next step is to choose the smoothing width T and sampling rate. The original time resolution of the raw data is 0.1 s and the smoothing operation has been applied to the raw data at different sampling rates of 0.1, 0.2, 0.3, 0.4, and 0.5, s. Figure 4 shows the raw and smoothed acceleration profiles at different sampling rates for a smoothing width of 0.5. It is observed that as the sampling rate increases, the spikes in the acceleration profiles are decreasing and observed to be smoother. Still, more smoother profiles can be obtained by increasing the sampling rate, but the real dynamics of the vehicles cannot be captured properly since the real data may be averaged out. Hence, the sampling rate is fixed as 0.5 s for further analysis. Some of the researchers also tried different smoothing width and adopted 0.5 s for smoothing process (Thiemann, Treiber, and Kesting 2008).

The plots of longitudinal speeds and accelerations are shown in Figure 5 for sample trajectories of the data set with raw data and smoothed data for the final values of 0.5 s sampling rate and 0.5 smoothing width. The effect of smoothing on speed and acceleration profiles can be clearly visualized in these figures.

Traffic Characteristics

The volume to capacity ratio (V/C ratio) of the collected traffic data is around 0.65, thatcorresponds to moderate traffic conditions. The traffic stream comprises 50% of two wheelers, 40% of cars and 10% of other categories (auto-rickshaws, buses, trucks, light commercial vehicles). For the calibration purpose, a total of 500 vehicle trajectories have been extracted. The statistics on longitudinal speeds of different categories of vehicles are given in the Table 1. The minimum speed of vehicles is zero due to the effect of downstream traffic signal.

Calibration methodology

The optimal parameters for the considered car-following models need to be obtained. The equations of the models (Equations 2 and 4) have non-linear acceleration functions corresponding to non-linear optimization problem that has to be solved numerically.

Simulation set-up

The observed gaps, speeds and accelerations can be compared with the simulated trajectories obtained by car-following models considering the leading vehicle as an externally controlled input. The simulation is initialized with the observed values from the data i.e., $v_{fol}^{sim}(t = 0) = v_{fol}^{data}(0); s_{fol}^{sim}(t = 0) = s_{fol}^{data}(0)$ and the input variables associated with the leader are always assigned from the observed data. Acceleration of the follower is computed using the car-following model, and its' speeds and positions are estimated using the equations of motion. The gap to the leading vehicle is obtained by calculating the difference between the simulated position (front bumper) of follower $x^{sim}(t)$ and the observed position (rear bumper) of the leader $x_{data}^{lead}(t)$:

$$S^{sim}(t) = x_{data}^{lead}(t) - x^{sim}(t) - l \tag{12}$$

where
$S^{sim}\ (t) = Simulated\ gap\ to\ the\ leading\ vehicle$,
$l = Length\ of\ leader$

This simulated gap can be directly compared with the observed gap $S^{obs}(t)$.

Objective function

The calibration process aims to minimize the difference between observed and simulated variable of interest. Any variable such as acceleration, speed, relative speed or relative distance can be used as the MoP. In this study, the gap between the front bumper of the follower and rear bumper of the leader (clear gap) has been used as the MoP for the objective function. The error between the simulated gap (s^{sim}) and observed gap (s^{obs}) is the quantitative measure needed for the objective function to perform parameter optimization. Three different error measures such as relative error, absolute error, and mixed error are considered for the calibration of car-following model. The formulations are given below:

$$S^{rel} = \frac{1}{n} \sum_{i=1}^{n} \left(\frac{s_i^{sim} - s_i^{obs}}{s_i^{obs}} \right)^2 \tag{13}$$

The relative error is weighted by the inverse of observed distance and this measure is more sensitive to small distances than to large distance. The absolute error measure is given by:

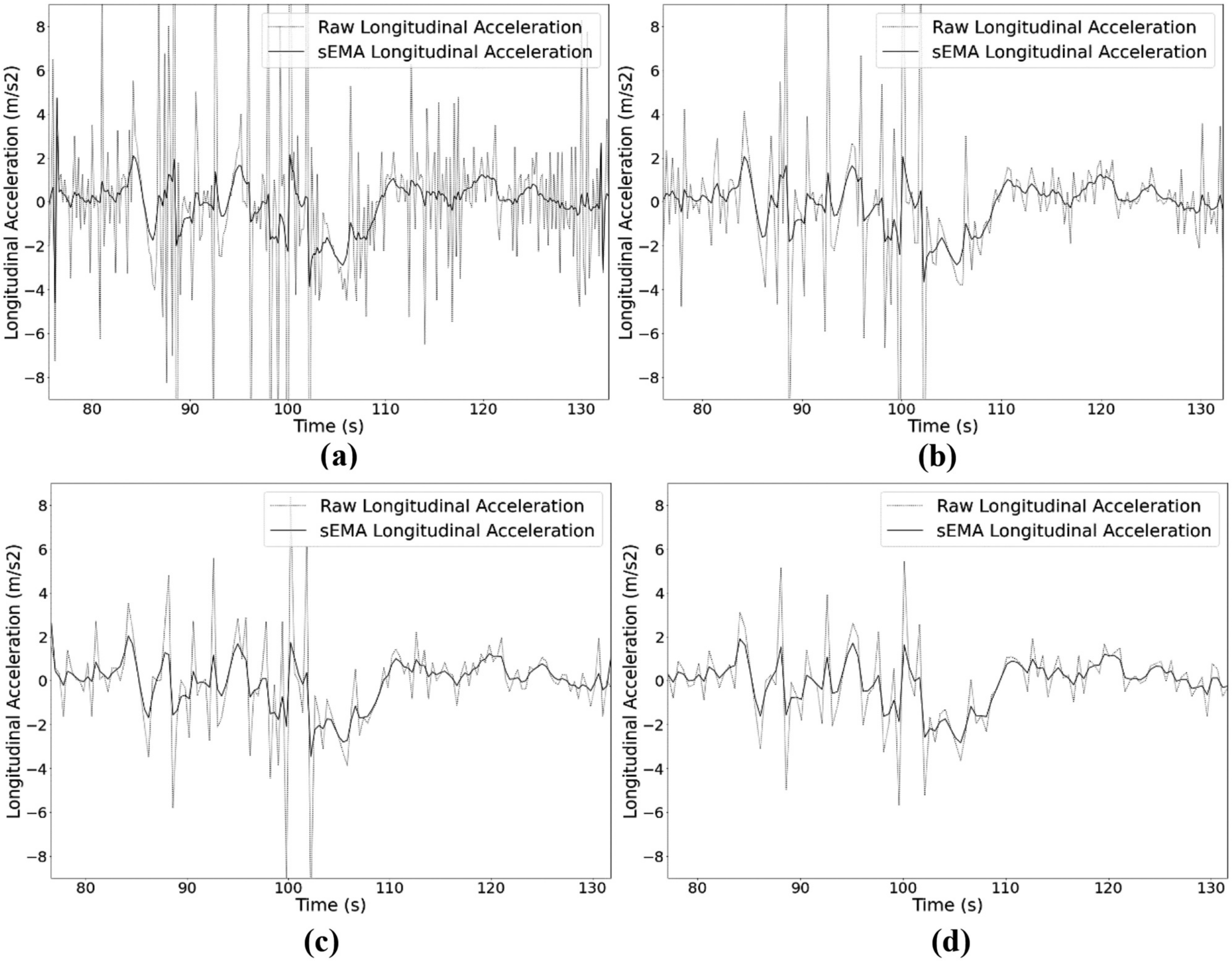

Figure 4. Raw and smoothed acceleration profiles at different sampling rates: a) 0.2 s, b) 0.3 s, c) 0.4 s, and d) 0.5 s at smoothing width 0.5.

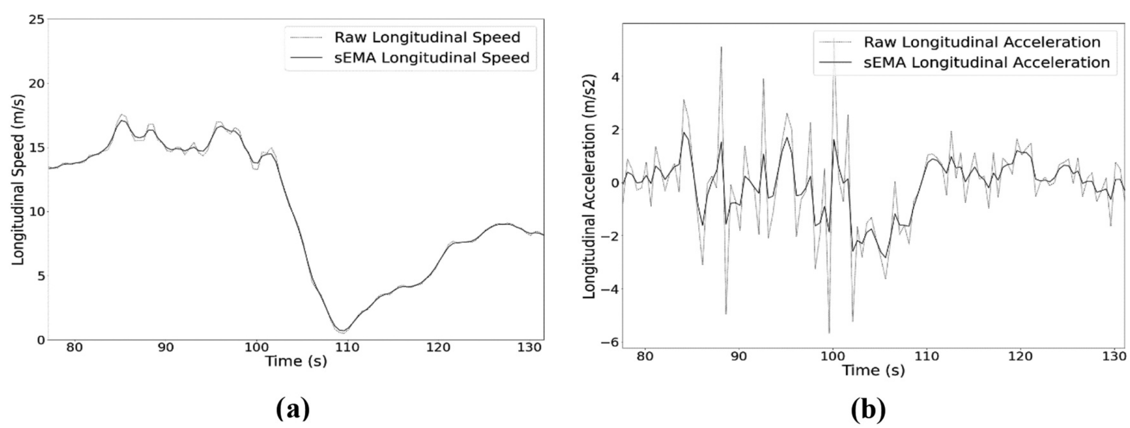

Figure 5. Raw data and smoothed a) longitudinal speed and b) longitudinal acceleration, at 0.5 sec sampling rate and 0.5 smoothing window.

$$S^{abs} = \frac{\sum_{i=1}^{n} \left(s_i^{sim} - s_i^{obs}\right)^2}{\sum_{i=1}^{n} \left(s_i^{obs}\right)^2} \tag{14}$$

In the case of absolute error, since the denominator is summated over the whole time series interval, it is less sensitive to slight deviations in the observed data. Nevertheless, the absolute error measure is more sensitive to significant differences for large distances. To overcome the limitations of these error functions, mixed error which is a combination of relative error and absolute error functions is also used:

$$S^{mix} = \frac{\sum_{i=1}^{n} \left(s_i^{sim} - s_i^{obs}\right)^2 / \left|s_i^{obs}\right|}{\sum_{i=1}^{n} \left|s_i^{obs}\right|} \tag{15}$$

Table 1. Speed characteristics of vehicles in the study section.

	Longitudinal Speed (m/s)		
Vehicle Type	Mean	Min.	Max.
TW	7.7	0.0	23.6
Car	7.7		29.3
Auto	6.9		15.7
LCV	6.2		17.5
Van	8.1		22.2
MCV	5.6		14.8
Bus/Truck	6.4		15.8

Optimization with genetic algorithm

To solve non-linear optimization problem, a popular evolutionary global search algorithm, genetic algorithm is applied. The process of implementation of genetic algorithm is explained here:

- An individual is a set of parameters of a car-following model and collection of N such individuals is population.
- Objective function (Equations 13, 14 or 15) is used to obtain the fitness score of the individuals in every iteration.
- Based on the value of fitness, two individuals (parents) are randomly selected and combined (crossover) to produce an offspring i.e., a new individual, which is then added to the population.
- Individuals, except those with high fitness values, will undergo mutations based on mutation probability.
- Modified population is considered as a new generation and is fed into the next iteration.

The algorithm is terminated based on the maximum number of iterations and the maximum iterations without improvement in the solution. The resulting solution contains the optimized value of parameters.

Boundary values of parameters

The optimization algorithm requires the possible range of parameter values to be predefined for an efficient search. The parameter constraints of the two car-following models considered for calibration have been adopted (Thiemann, Treiber, and Kesting 2008) as follows:

- IDM parameters: Desired Speed (v_0) = [1, 30] m/s; Minimum Spacing (s_0) = [0.1, 8] m; Maximum Acceleration (a) = [0.1, 6] m/s^2; Comfortable Deceleration (b) = [0.1, 6] m/s^2; Desired Time Gap (T) = [0.1, 5] s; Acceleration exponent (δ) = [1, 40]
- FVDM parameters: Desired Speed (v_0) = [1, 30] m/s; Transition Width (Δs) = [0.1, 10]; Form Factor (β) = [0.1, 10]; Adaption time (τ) = [0.05, 20] s; Sensitivity Coefficient (γ) = [0, 3].

In addition to the above constraints, the backward movement of vehicles in the simulation has been eliminated by setting the negative simulated speeds to zero. Also, in case of FVDM, some set of parameters may lead to collision (negative spacing) during simulation and hence, a huge penalty has been added to the objective function, so that the optimization algorithm would not consider such solutions to be optimal.

Calibration results

Extraction of leader-follower pairs

The smoothed trajectory data has been further processed to extract the leader-follower pairs. The car-following periods of leader-follower pairs are identified based on the following criteria:

- Leader should be present in front of the follower and should laterally overlap with the follower.
- Lateral gap with nearest non-overlapping leaders and adjacent vehicles should be at least 1 m (Mallikarjuna, Tharun, and Pal 2013) to suppress the interactions from surrounding vehicles.
- Duration of following time should be at least 12 seconds (Zhu et al. 2018; Anand et al. 2019) to ensure that the car-following stayed long enough to be analyzed.

The vehicles moving without an overlapping leader and not being influenced significantly by the other surrounding vehicles (within 1 m lateral gap) are considered to be without leaders. The trajectories of the pairs satisfying the above criteria are plotted to assure the following behavior through visualization (Figure 6). Then, the starting and terminating time step of each following periods is recorded. The pairs exhibited different driving regimes such as steady state following (Figure 6a), shying away (Figure 6b), approaching, and stopping (Figure 6c). The vehicles without leaders have also been considered for calibration (Figure 6d). The acceleration values beyond the range of ±4 m/s^2 (within which most of the data points are present) are removed after selecting the car-following samples from the dataset to avoid unrealistic values.

Car-following periods for analysis

The present study is carried out to calibrate car-following models for urban arterial roads. A total of around 500 trajectories have been extracted from the videos recorded in the study stretch. It is possible that the same leader-follower pair may have multiple car-following periods. Each of those segments is considered as a sample car-following period. 86 car-following periods are obtained from the trajectory data, satisfying the criteria of car-following behavior. The dominant class wise leader-follower pairs in the trajectory data are Car-Car (23) and TW-Car (12).

Optimal parameters

IDM

The calibration results for the IDM model considering three objective functions, relative error, mixed error and absolute error (Equations 13 to **15**) are presented in Table 2. The obtained errors are in the range of 2.5% to 9%, which agrees with the earlier studies of the IDM model (Kurtc and Treiber 2016) and it is observed that the variations in parameter values for different objective functions is not much significant. The desired speed values obtained are approximately 61 kmph (17 m/s), which are (1) lesser than desired speed values obtained in previous studies under homogeneous traffic conditions (Ciuffo, Punzo, and Montanino 2014). The possible reason is that the traffic stream consists of combination of both fast moving and slow-moving vehicles (wide mix of vehicles), which results in lower desired speed values, (2) higher than desired speed values (approximately 40 kmph) reported in a previous study under disordered (Indian) traffic conditions (Raju, Arkatkar, and Joshi 2020).

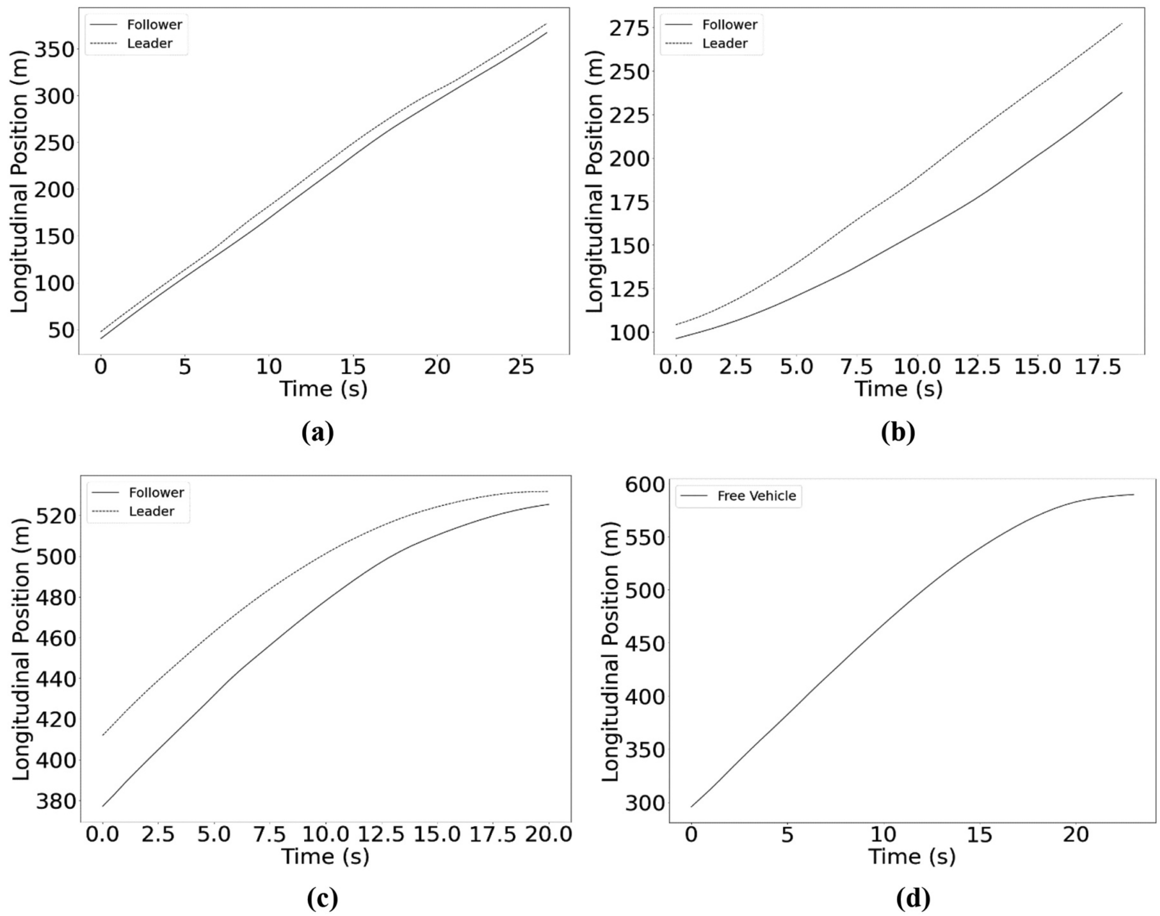

Figure 6. Following periods extracted from trajectory data – Sample of few leader-follower pairs representing (a) steady state following (b) shying away (c) approaching and (d) vehicle without leader and approaching signal.

This can be attributed due to fact that the vehicular composition in the study section has higher proportion of cars (40%) as compared to the earlier study (27%).

The values of minimum spacing (0.27 to 0.5 m) and desired time gap values (0.24 to 0.38 s) are lower when compared with the earlier studies in homogeneous traffic conditions (Kesting and Treiber 2008; Ciuffo, Punzo, and Montanino 2014). Vehicles moving under non-lane discipline traffic conditions, tend to keep lesser headways with the leaders and seek for an opportunity to overtake or perform lateral shift (wherever gaps are available) which would result in lower values, or this could be the result of data incompleteness which means that representative samples are needed for each regime: cruising, free flow, approaching, standstill, etc. Moreover, this needs to be further investigated with more following samples composed of different types of leader-follower pairs. The other parameters agree with earlier studies under homogeneous and disordered traffic conditions. Acceleration exponent values (1.03 to 3.42) obtained are found to be reasonable in disordered traffic.

It is observed that among the three objective functions, the absolute error function gives the value of 2.77% whereas the relative error function gives an error value of 8.85%. Since, mixed error is a combination of relative and absolute error, it is not sensitive to the difference between the observed and simulated gaps. Hence, the optimal parameter values obtained with respect to mixed error function are used for simulating the longitudinal gaps of follower with respect to the leader.

FVDM

The calibration results of FVDM by considering three objective functions are given in Table 1. The objective function values are in the range 8.5% to 19.5%. In the case of FVDM, few parameter values across different objective functions vary, unlike IDM. This shows that for the disordered traffic data considered, the parameters of FVDM are more sensitive to error functions, in comparison with the IDM parameters. Both IDM and FVDM models exhibit similar desired speed values which are consistent.

The adaption time values (0.3 to 0.58) are very less when compared with homogeneous traffic conditions (Kesting and Treiber 2008). This is because drivers exhibit aggressive behavior and react quickly to adapt optimal speed, particularly two wheelers. Further investigation along these lines needs to be done. Transition width (3.64 to 5.68 m) are observed to be lesser compared to homogeneous traffic (Kesting and Treiber 2008). This implies that the vehicles in disordered traffic have higher optimum speed for the same form factor and spacing compared to homogeneous traffic. Vehicles often perform lane changes or lateral shifts whenever it is possible and maintain higher speeds, especially two wheelers because of their higher maneuverability. The above results may also be due to data incompleteness which needs to be further explored.

The parameter, form factor values agree with the values reported in earlier studies. Figure 7 shows the comparison of the simulated gap resulting from the calibrated parameters of IDM and FVDM models with the observed gap. Figure 7a

Table 2. Optimal parameters from calibration of IDM and FVDM.

Parameters		Boundary values	Relative Error	Mixed Error	Absolute Error
IDM					
Error (%)	-	-	8.85	4.24	2.77
Desired Speed (m/s)	V0	[1,30]	17.35	17.79	15.26
Minimum Spacing (m)	S0	[0.1,8]	0.27	0.34	0.5
Comfortable Deceleration (m/s^2)	b	[0.1,6]	0.53	0.47	0.68
Maximum Acceleration (m/s^2)	a	[0.1,6]	0.81	0.88	0.84
Desired Time Gap (s)	T	[0.1,5]	0.38	0.29	0.24
Acceleration exponent	δ	[1,40]	3.42	1.03	1.82
FVDM					
Error (%)	-	-	19.31	12.4	8.57
Desired Speed (m/s)	V0	[1,30]	17.56	16.18	15.31
Transition Width (m)	ΔS	[0.1,10]	5.68	5.62	3.64
Form Factor	β	[0.1,10]	0.75	1.2	2.44
Adaption Time (s)	τ	[0.05,20]	0.3	0.62	0.58
Sensitivity coefficient	γ	[0,3]	1.59	0.61	0.74

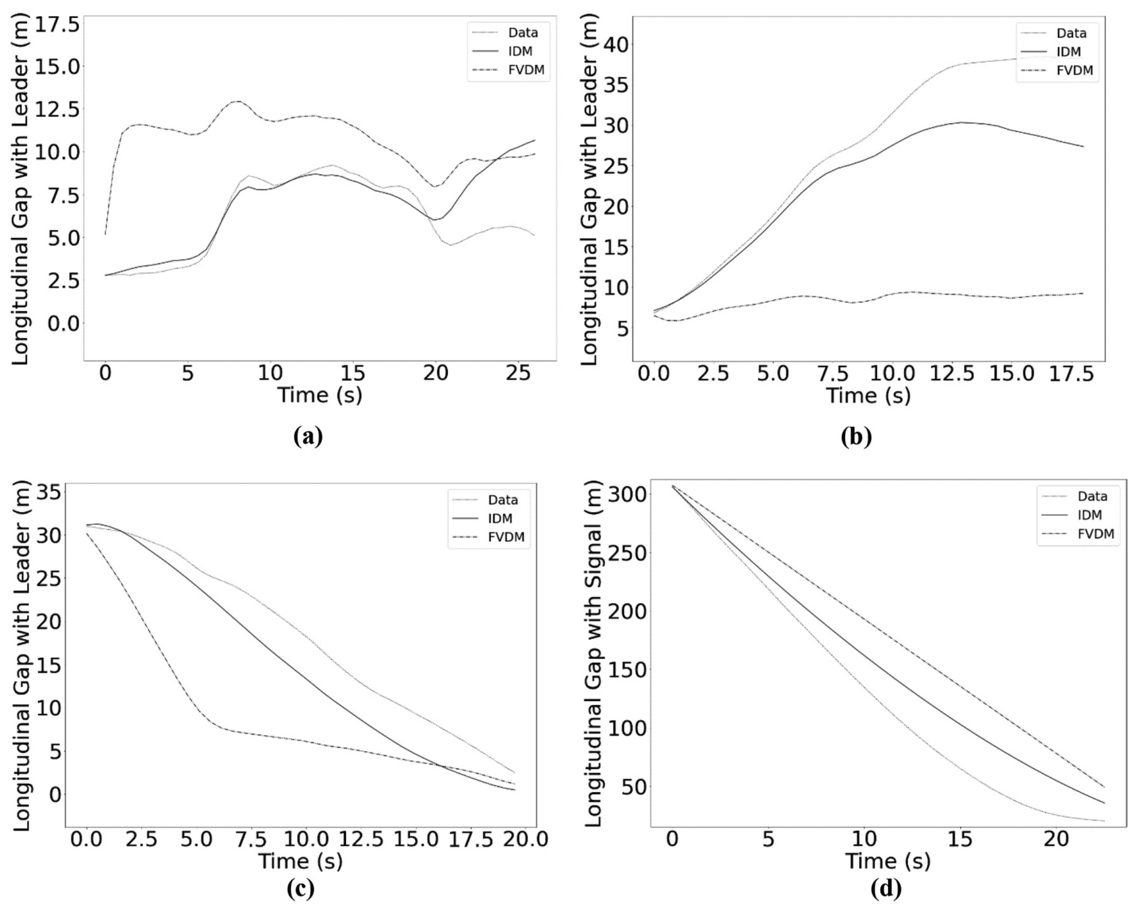

Figure 7. Observed and predicted gaps (based on mixed error function) with IDM and FVDM for representing (a) steady state following (b) shying away (c) approaching and (d) vehicle without leader and approaching signal.

represents the car-following pairs in steady state, Figure 7b represents the shying away behavior during following, where the gap increases with time and the approaching behavior is observed in Figure 7c. The observed and simulated gaps of a vehicle moving without leader approaching traffic signal is shown in Figure 7d. It can be observed from the figures that IDM is better fit for all the scenarios compared to FVDM.

Compared to the FVDM, the IDM has significantly smaller errors (4.24%), which implies that it could perform better than the FVDM in different traffic situations. Therefore, the IDM is a more suitable car-following model for microscopic traffic simulation tools in disordered traffic, which is also supported by other literature. However, from the microscopic perspective, any car-following model with errors between approximately 15 and 25% can be used (Brockfeld and Wagner 2005). These errors probably may be due to random component in driver behavior which means certain behavior cannot be predicted and has no noticeable pattern.

Summary and conclusions

The present study aims to investigate car-following models such as Intelligent Driver Model (IDM) and Full Velocity Difference Model (FVDM) in disordered traffic using trajectory data collected from an urban arterial road in Chennai city, India using Unmanned Air Vehicles. The raw trajectory data has been smoothed using Symmetrical Exponential Moving Average technique to remove the noises. The car-following pairs are extracted from the trajectories based on lateral overlap, and following period. The optimal parameters of the IDM and FVDM are obtained using Genetic Algorithm considering spacing between leader and follower as the measure of performance in the objective function. The optimization is carried out based on three different objective functions i.e., error measures. Calibration errors are obtained in the range of 2.5%–19.5%, and these results are consistent with the range of errors obtained in previous studies. The optimal parameter values of minimum spacing and desired time gap in IDM, and adaptation time and transition width in FVDM are found to be lesser compared to homogeneous traffic conditions. This is believed to be due to ease in lateral shift, driver aggressiveness, maintaining lesser gaps and higher maneuverability of two wheelers or these values may be obtained due to data incompleteness. This needs further examination with more datasets that consists of all traffic regimes. Other parameters of the models are found to be logical and consistent. The comparison of observed and simulated gaps shows that both IDM and FVDM produces trajectories that are closer to observed data However, IDM performs better than FVDM in predicting the following behavior of vehicles in disordered traffic.

The models such as IDM and FVDM have been frequently used in microscopic traffic modeling of homogeneous traffic. However, the application of these models under disordered traffic to model car-following behavior of vehicles is still under investigation. The present study in an initial step toward it, in order to obtain the useful insights on evaluating the suitability of these models and to find solution for data issues. The present study can be further extended by considering different parameters for dominating vehicle categories in the traffic stream to capture the variations in their behavior which in turn will improve the accuracy of simulation models.

The adopted methodology can also be applied to calibrate other car-following models to explore the suitability of better models for disordered traffic. Moreover, the calibration can be performed with different datasets collected from other locations to address the data transferability issues. The study of car-following behavior considering different parameters for different regimes is the another challenging research problem which can be addressed as a further scope of the present study.

Disclosure statement

No potential conflict of interest was reported by the author(s).

References

Anand, P. A., P. Atmakuri, V. S. R. Anne, G. Asaithambi, K. K. Srinivasan, R. Sivanandan, and B. R. Chilukuri. 2019. "Calibration of vehicle-following Model Parameters Using Mixed Traffic Trajectory Data." *Transportation in Developing Economies* 5 (2): 1–11. doi:10.1007/s40890-019-0086-4.

Asaithambi, G., V. Kanagaraj, K. K. Srinivasan, and R. Sivanandan. 2018. "Study of Traffic Flow Characteristics Using Different vehicle-following Models under Mixed Traffic Conditions." *Transportation Letters* 10 (2): 92–103. doi:10.1080/19427867.2016.1190887.

Bando, M., K. Hasebe, K. Nakanishi, A. Nakayama, A. Shibata, and Y. Sugiyama. 1995. "Phenomenological Study of Dynamical Model of Traffic Flow." *Journal de Physique I* 5 (11): 1389–1399. doi:10.1051/jp1:.

Brackstone, M., and M. McDonald. 1999. "Car-following: A Historical Review." *Transportation Research. Part F, Traffic Psychology and Behaviour* 2 (4): 181–196. doi:10.1016/S1369-8478(00.

Bradski, G., and A. Kaehler. 2008. *Learning OpenCV: Computer Vision with the OpenCV Library.* " (United States: O'Really Media, Inc.,).

Brockfeld, E., and P. Wagner. 2005. "Calibration and Validation of Microscopic Traffic Flow Models." In Hoogendoorn, S. P., Luding, S., Bovy, P. H. L., Schreckenberg, M., Wolf, D. E. *Traffic and Granular Flow'03*, 67–72. Berlin, Heidelberg: Springer. doi:10.1007/3-540-28091-X_6.

Chandler, R. E., R. Herman, and E. W. Montroll. 1958. "Traffic Dynamics: Studies in Car following." *Operations Research* 6 (2): 165–184. doi:10.1287/opre.6.2.165.

Ciuffo, B., V. Punzo, and M. Montanino. 2014. "Global Sensitivity Analysis Techniques to Simplify the Calibration of Traffic Simulation Models. Methodology and Application to the IDM car-following Model." *IET Intelligent Transport Systems* 8 (5): 479–489. doi:10.1049/iet-its.2013.0064.

Daamen, W., M. Campanella, and S. P. Hoogendoorn. 2013. "Calibration of Nomad Parameters Using Empirical Data." In Kozlov Alexander S. Bugaev, Marina V. Yashina, Andreas Schadschneider, Michael Schreckenberg, V. V., Buslaev, A. P., Bugaev, A. S., Yashina, M. Y., Schadschneider, A., Schreckenberg, M.*Traffic and Granular Flow'11*, 109–120. Berlin, Heidelberg: Springer.

Ge, H. X., R. J. Cheng, and Z. P. Li. 2008. "Two Velocity Difference Model for a Car Following Theory." *Physica A: Statistical Mechanics and Its Applications* 387 (21): 5239–5245. doi:10.1016/j.physa.2008.02.081.

Gipps, P. G. 1981. "A Behavioural car-following Model for Computer Simulation." *Transportation Research Part B: Methodological* 15 (2): 105–111. doi:10.1016/0191-2615(81).

Heyes, M. P., and R. Ashworth. 1972. "Further Research on car-following Models." *Transportation Research* 6 (3): 287–291. doi:10.1016/0041-1647(72)90020-2.

Jiang, R., Q. Wu, and Z. Zhu. 2001. "Full Velocity Difference Model for a car-following Theory." *Physical Review E* 64 (1): 017101. doi:10.1103/PhysRevE.64.017101.

Jin, S., D. Wang, P. Tao, and P. Li. 2010. "Non-lane-based Full Velocity Difference Car following Model." *Physica A: Statistical Mechanics and Its Applications* 389 (21): 4654–4662. doi:10.1016/j.physa.2010.06.014.

Kanagaraj, V., G. Asaithambi, T. Toledo, and T. C. Lee. 2015. "Trajectory Data and Flow Characteristics of Mixed Traffic." *Transportation Research Record* 2491 (1): 1–11. doi:10.3141/2491-01.

Kesting, A., and M. Treiber. 2008. "Calibrating car-following Models by Using Trajectory Data: Methodological Study." *Transportation Research Record* 2088 (1): 148–156. doi:10.3141/2088-16.

Kometani, E. 1959. "Dynamic Behavior of Traffic with a Nonlinear spacing-speed Relationship." In *Proceedings of the Symposium on Theory of Traffic Flow* (Research Laboratory, General Motors Corp.: Elsevier Publishing Co. pp.), 105–119.

Krajewski, R., J. Bock, L. Kloeker, and L. Eckstein (2018). The Highd Dataset: A Drone Dataset of Naturalistic Vehicle Trajectories on German Highways for Validation of Highly Automated Driving Systems. In *2018 21st International Conference on Intelligent Transportation Systems (ITSC)*, 2118–2125. IEEE. doi: 10.1109/ITSC.2018.8569552

Kurtc, V., and M. Treiber. 2016. "Calibrating the Local and Platoon Dynamics of car-following Models on the Reconstructed NGSIM Data." In Victor, L. K., Winnie, D. *Traffic and Granular Flow'15*, 515–522. Cham: Springer.

Kurtc, V. 2020. "Studying car-following Dynamics on the Basis of the HighD Dataset." *Transportation Research Record* 2674 (8): 813–822. doi:10.1177/0361198120925063.

Mallikarjuna, C., B. Tharun, and D. Pal. 2013. "Analysis of the Lateral Gap Maintaining Behavior of Vehicles in Heterogeneous Traffic Stream." *Procedia-social and Behavioral Sciences* 104: 370–379. doi:10.1016/j.sbspro.2013.11.130.

May, A. D., and H. E. Keller. 1967. "Non-integer car-following Models." *Highway Research Record* 199 (1): 19–32.

NGSIM, U. 2005. *101 Data Analysis: SUmmary Report* (Washington, DC: Federal Highway Administration).

Ossen, S., and S. P. Hoogendoorn. 2005. "Car-following Behavior Analysis from Microscopic Trajectory Data." *Transportation Research Record* 1934 (1): 13–21. doi:10.1177/0361198105193400102.

Raju, N., S. Arkatkar, and G. Joshi. 2020. "Evaluating Performance of Selected Vehicle following Models Using Trajectory Data under Mixed Traffic Conditions." *Journal of Intelligent Transportation Systems* 24 (6): 617–634. doi:10.1080/15472450.2019.1675522.

Ranjitkar, P., T. Nakatsuji, and A. Kawamua. 2005. "Car-following Models: An experiment-based Benchmarking." *Journal of the Eastern Asia Society for Transportation Studies* 6: 1582–1596. doi:10.11175/easts.6.1582.

Ravishankar, K. V. R., and T. V. Mathew. 2011. "Vehicle-type Dependent car-following Model for Heterogeneous Traffic Conditions." *Journal of Transportation Engineering* 137 (11): 775–781. doi:10.1061/(ASCE)TE.1943-5436.0000273.

Saifuzzaman, M., Z. Zheng, M. M. Haque, and S. Washington. 2015. "Revisiting the Task–Capability Interface Model for Incorporating Human Factors into car-following Models." *Transportation Research Part B: Methodological* 82: 1–19. doi:10.1016/j.trb.2015.09.011.

Thiemann, C., M. Treiber, and A. Kesting. 2008. "Estimating Acceleration and lane-changing Dynamics from Next Generation Simulation Trajectory Data." *Transportation Research Record* 2088 (1): 90–101. doi:10.3141/2088-10.

Treiber, M., A. Hennecke, and D. Helbing. 2000. "Microscopic Simulation of Congested Traffic Helbing, D., Hermann, H., Schreckenberg, M., Wolf, D. E." In *Traffic and Granular Flow'99*, 365–376. Berlin, Heidelberg: Springer. doi:10.1007/978-3-642-59751-0_36.

Treiber, M., and A. Kesting. 2013. "Traffic Flow Dynamics: Data, Models and Simulation." *Physics Today* 67 (3): 54. doi:10.1007/978-3-642-32460-4.

Wiedemann, R. 1974. *Simulation des Straßenverkehrsflusses (1974th ed.)*. Karlsruhe, Germany: Institut für Verkehrswesen der Universität.

Zheng, Y., S. He, R. Yi, F. Ding, B. Ran, P. Wang, and Y. Lin. 2020. "Categorizing car-following Behaviors: Wavelet-based Time Series Clustering Approach." *Journal of Transportation Engineering, Part A: Systems* 146 (8): 04020072. doi:10.1061/JTEPBS.0000402.

Zhu, M., X. Wang, A. Tarko, and S. Fang. 2018. "Modeling car-following Behavior on Urban Expressways in Shanghai: A Naturalistic Driving Study." *Transportation Research Part C: Emerging Technologies* 93: 425–445. doi:10.1016/j.trc.2018.06.009.